High nuclear polarization of helium-3 at low and high pressure by metastability exchange optical pumping at 1.5 Tesla

Marie Abboud, Alice Sinatra, Xavier Maître, Geneviève Tastevin, Pierre-Jean Nacher

High nuclear polarization of ^{3}He at low and high pressure by metastability exchange optical pumping at 1.5 Tesla

M. Abboud, A. Sinatra, X. Maître*, G. Tastevin, P.-J. Nacher
marie.abboud@lkb.ens.fr,alice.sinatra@lkb.ens.fr
Laboratoire Kastler Brossel - Ecole Normale Supérieure, 24 rue Lhomond, 75005 Paris, France [1]
* *U2R2M, Université Paris-Sud and CIERM - Hôpital de Bicêtre, 94275 Le Kremlin-Bicêtre Cedex, France* [2]

Abstract Metastability exchange optical pumping of helium-3 is performed in a strong magnetic field of 1.5 T. The achieved nuclear polarizations, between 80% at 1.33 mbar and 25% at 67 mbar, show a substantial improvement at high pressures with respect to standard low-field optical pumping. The specific mechanisms of metastability exchange optical pumping at high field are investigated, advantages and intrinsic limitations are discussed. From a practical point of view, these results open the way to alternative technological solutions for polarized helium-3 applications and in particular for magnetic resonance imaging of human lungs.

1 Introduction

A gas of ground state ^{3}He atoms in which a high degree of nuclear polarization is achieved offers an incredibly rich playground in various fields of science, from statistical or nuclear physics to biophysics and medicine [1]. Depending on the targeted application, the degree of nuclear polarization, the sample density, or the production rate of polarized atoms should be optimized. A recent application, which may have an important impact on the diagnosis of pulmonary diseases, is polarized gas magnetic resonance imaging (MRI) [2]. Clinical studies to demonstrate the relevance of this new tool are under way in Europe and in the United States. Yet, if a wide expertise exists in MRI to adapt the existing imaging techniques to the case of polarized gases, the gas preparation remains a critical stage to be transferred from physics laboratories to hospitals. Two methods are presently used to polarize ^{3}He: spin-exchange with optically pumped alkali atoms [3] and pure-He metastability exchange optical pumping (MEOP) [4]. In standard conditions, MEOP is performed at low pressures (1 mbar) in a guiding magnetic field of the order of 1 mT. Circularly polarized light at 1083 nm, corresponding to the 2^3S-2^3P transition of ^{3}He, is used to transfer angular momentum to the atoms and nuclear polarization is created by hyperfine coupling in the metastable 2^3S state. Through metastability exchange collisions, nuclear polarization builds up in the ground state. The steady-state nuclear polarization obtained by MEOP in standard conditions rapidly decreases if the pressure of the sample exceeds a few mbar (see below, Fig.5-a) [5, 6, 7]. Therefore a delicate polarization-preserving compression stage is necessary for MRI where the gas should be at atmospheric pressure for inhalation, and for all applications needing a dense sample. In this letter, the MEOP scheme is shown to withstand large hyperfine decoupling. A strong magnetic field of 1.5 T actually improves its performances with respect to standard low-field optical pumping. At 1.33 mbar, high nuclear polarizations

[1] Laboratoire Kastler Brossel is a unité de recherche de l'Ecole Normale Supérieure et de l'Université Pierre et Marie Curie, associée au CNRS (UMR 8552).

[2] U2R2M (Unité de Recherche en Résonance Magnétique Médicale) is a unité de recherche de l'Université Paris-Sud, associée au CNRS (UMR 8081)

of the order of 80% are routinely obtained with much lighter experimental constraints. At higher pressures, the achieved nuclear polarizations are dramatically increased compared to published low-field results. An elementary model with simple rate equations is used to account for these results.

2 Experimental setup and methods

Experiments are performed in the bore of the 1.5 T superconducting magnet of a clinical MRI system. The experimental apparatus is sketched in Fig.1. The helium gas is enclosed in

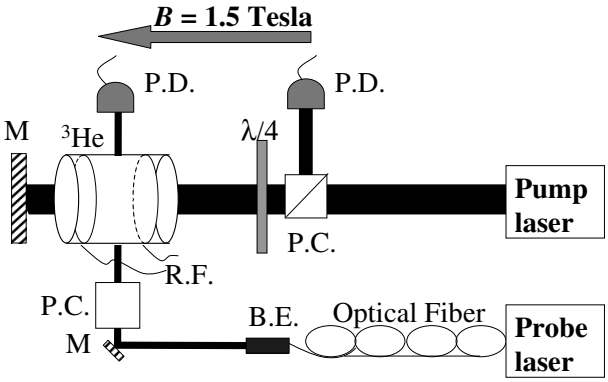

Figure 1: Experimental setup. The nuclear polarization is measured by the absorption of a transverse probe beam. B: static magnetic field, P.D.: photodiode, P.C.: polarizing beam-splitter, B.E: beam expander, $\lambda/4$: quarter wave plate, M: mirror, R.F.: radio-frequency to excite the discharge.

a sealed cylindrical Pyrex cell (diameter 5 cm, length 5 cm). Four cells filled with 1.33 mbar, 8 mbar, 32 mbar and 67 mbar of pure ^{3}He are used. A radio-frequency discharge at 3 MHz is sustained in the gas by external electrodes, leading to metastable atom densities n_m in the 0.3-3 $\times 10^{10}$atoms/cm^3 range, depending on the applied voltage and on the gas pressure. The optical pumping laser is either a 50 mW single mode laser diode amplified to 0.5 W [8], or a broadband fiber laser (1.63 GHz FWHM) delivering 2 W [9]. The pump beam is back-reflected to enhance its absorption, which is monitored on the transmitted beam with a photodiode. At the entrance of the cell, the Gaussian transverse intensity profile of the pump beam has a FWHM of the order of 2 cm. A weak probe beam from a single mode laser diode is used to measure the nuclear polarization. It is linearly polarized perpendicularly to the magnetic field (σ polarization). The discharge intensity is modulated at 133 Hz, and the probe absorption is measured with a lock-in amplifier. Laser sources and electronics remain several meters away from the magnet bore, in a low-field region.

At 1.5 T, due to Zeeman splitting, the energy levels of the 2^3S and 2^3P states are spread over 80 and 160 GHz respectively (Fig.2-a). Hyperfine decoupling in the 2^3S state is significant, so that the eigenstates of the Hamiltonian show only little mixing between different eigenstates $|m_J, m_I\rangle$ of the decoupled spin system, where m_J, m_I, and m_F denote the magnetic quantum numbers for the electronic, nuclear, and total angular momentum, respectively. As shown in Fig.2-a, the 2^3S sublevels are arranged into three pairs of quasi-degenerate levels of increasing energies (A_1,A_2), (A_3,A_4), and (A_5,A_6) that correspond respectively to m_J=−1, 0, and 1 in the completely decoupled limit $B \rightarrow \infty$. For more details about the 2^3S level structure and the analytical expressions of eigenstates and energies, we refer the reader to [10]. The absorption spectra at low magnetic field and at 1.5 T

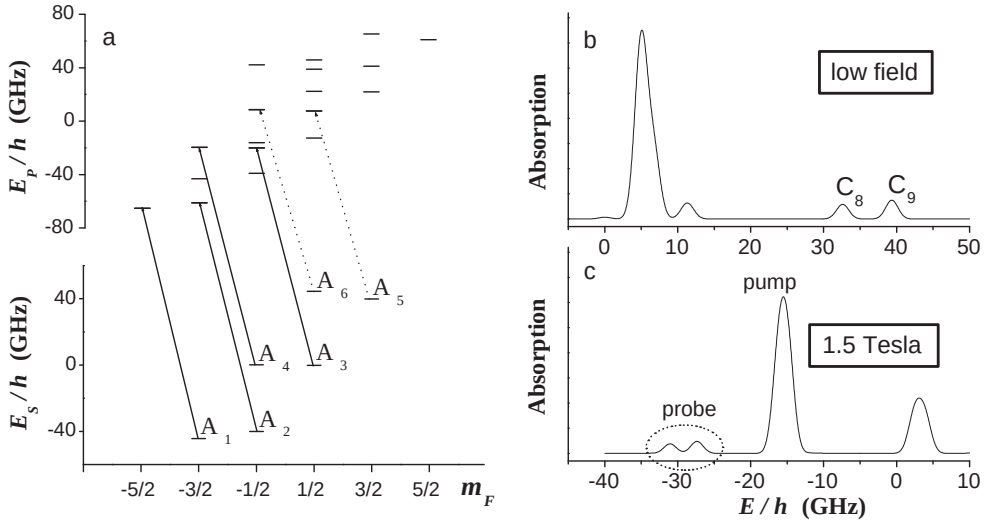

Figure 2: (a): Energies of the ^{3}He sublevels at 1.5 T for the metastable 2^3S state (E_S) and the 2^3P state (E_P). The transitions induced by the σ^--polarized pump (solid lines) and probe (dashed lines) are displayed. Each pump transition has a matrix element T_{ij} close to 1[10]. (b): Absorption spectrum at low magnetic field. (c): Absorption spectrum for σ^- light at 1.5 T. Vertical and horizontal scales are identical in Fig.2-b and c. Level names A_1 to A_6, energy zeroes and spectral line positions are defined as in reference [10].

are displayed in Figs.2-b and c, respectively. In standard MEOP, very high nuclear polarizations are obtained using C_8 or C_9 lines [6, 11]. Comparable polarizations are achieved at 1.5 T using the σ^--strong pump line displayed in Fig.2-c. All the results presented in this work are obtained with this pump transition. The performances and efficiencies of other optical pumping transitions at 1.5 T will be reported elsewhere. The pump simultaneously addresses the four 2^3S sublevels A_1 to A_4. Population transfer into the pair (A_5,A_6) is achieved by the following sequence : laser excitation, collisional redistribution in the 2^3P state and spontaneous emission. The ground state nuclear polarization M is defined as $M=(n_+ - n_-)/(n_+ + n_-)$ where n_+ and n_- denote populations of the m_I=1/2 and m_I=$-1/2$ nuclear spin states, respectively. In the absence of optical pumping, metastability exchange collisions impose a spin temperature distribution for the 2^3S sublevel populations, proportionally to $e^{\beta m_F}$ where $e^{\beta}=n_+/n_-=(1+M)/(1-M)$ [10]. The populations of sublevels A_5 and A_6, not addressed by the pump, are probed to measure M. Examples of probe absorption spectra for an unpolarized and an optically-pumped steady-state situation are shown in Fig.3-a. M is inferred from the relative heights of the absorption peaks. The build-up of the polarization, as well as its decay when the pump is turned off, are monitored by tuning the probe laser frequency on the probe transition starting from the A_5 (m_F=3/2) sublevel (Fig.3-b). These measurement procedures operate at arbitrary magnetic field and pressure [10].

3 Results

The steady-state polarization M_{eq} and the polarization build-up time constant t_b in the 1.33 mbar cell are shown in Figs.4-a and b as a function of the discharge-induced decay time T_1. Over a wide range of moderate to weak discharges (T_1 ranging from 300 s to

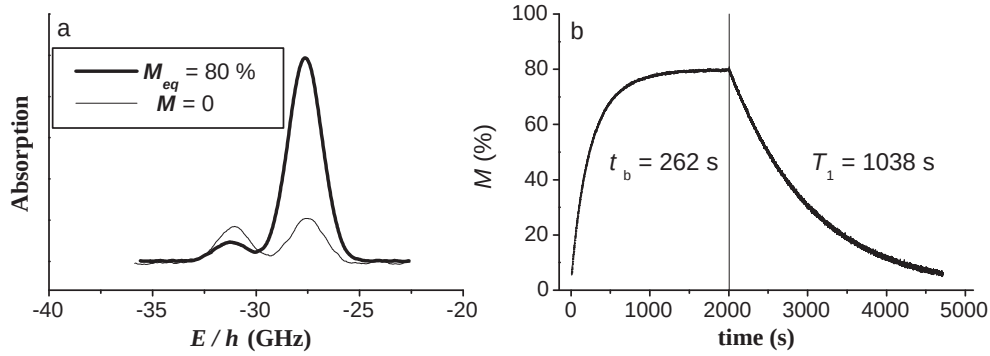

Figure 3: Examples of recorded signals in the 1.33 mbar cell: a- Absorption measurements on transitions from sublevels A_5 (E/h=-27.36 GHz) and A_6 (E/h=-31.04 GHz) at thermal equilibrium ($M \simeq 0$) and at steady-state nuclear polarization ($M=M_{eq}$) in an optically-pumped gas. b- Polarization build-up and discharge-induced decay deduced from changes of light absorption in sublevel A_5. Pump laser is applied at time t=0, and turned off after 2000 s.

1500 s), t_b (ranging from 60 to 350 s) is proportional to T_1 and the polarization achieved with the broadband 2 W laser is high, about 80%, independently of T_1. This behavior is specific to the high-field optical pumping, and contrasts with the standard low-field situation where a very weak discharge is required to obtain such large nuclear polarizations. For the strongest discharges, build-up times decrease (t_b ranging from 15 to 55 s) and steady-state polarizations are lower. Fig.4-c and d show the influence of the pump laser power for a given discharge (T_1=300 s). A laser power as low as 0.5 W is sufficient for the polarization and the build-up time to almost reach their asymptotic values. Similar studies of MEOP have been performed at higher pressures, where T_1 between 300 and 2600 s are measured. Selected results for a weak and a strong discharge at full laser power are shown in Fig.5 together with published low-field results. The polarizations obtained at high pressures are, to our knowledge, record MEOP values. The polarization build-up times weakly depend on ^{3}He pressure, in contrast with low-field MEOP [6, 12].

4 Discussion

An extension of the detailed model for standard MEOP [11] to high-field conditions [10] is required to compute the populations of all atomic sublevels. Here, for simplicity, an elementary model is used to account for the main observed features. We assume that (*i*) atoms are fully pumped into the (A_5,A_6) pair, and (*ii*) the populations of sublevels not addressed by the pump laser are imposed by the ground state spin temperature which only depends on M: a_5=$(1+M)/2$ and a_6=$(1-M)/2$. The sublevel A_5 is totally oriented (m_J=1, m_I=1/2) and carries a nuclear angular momentum $\langle I_z\rangle$=$\hbar/2$, while A_6 has a small component on (m_J=0, m_I=1/2) and a large component on (m_J=1, m_I=-1/2) and thus carries a nuclear angular momentum $\langle I_z\rangle$=$\hbar(\epsilon-1)/2$ with ϵ=1×10^{-2} at 1.5 T [13]. The rate equation for M, resulting from relaxation and metastability exchange, is then:

$$\frac{dM}{dt} = \frac{2\langle I_z\rangle/\hbar - M}{T_e} - \frac{M}{T_1} \qquad \text{with} \qquad \langle I_z\rangle = \frac{\hbar}{2}(M + \epsilon\frac{1-M}{2})\,,$$

where $1/T_e$ is the metastability exchange collision rate for a ^{3}He atom in the ground state ($1/T_e$=$n_m\times1.53\times10^{-10}$cm^3/s), and $2\langle I_z\rangle/\hbar$ is the nuclear polarization in the 2^3S state. One

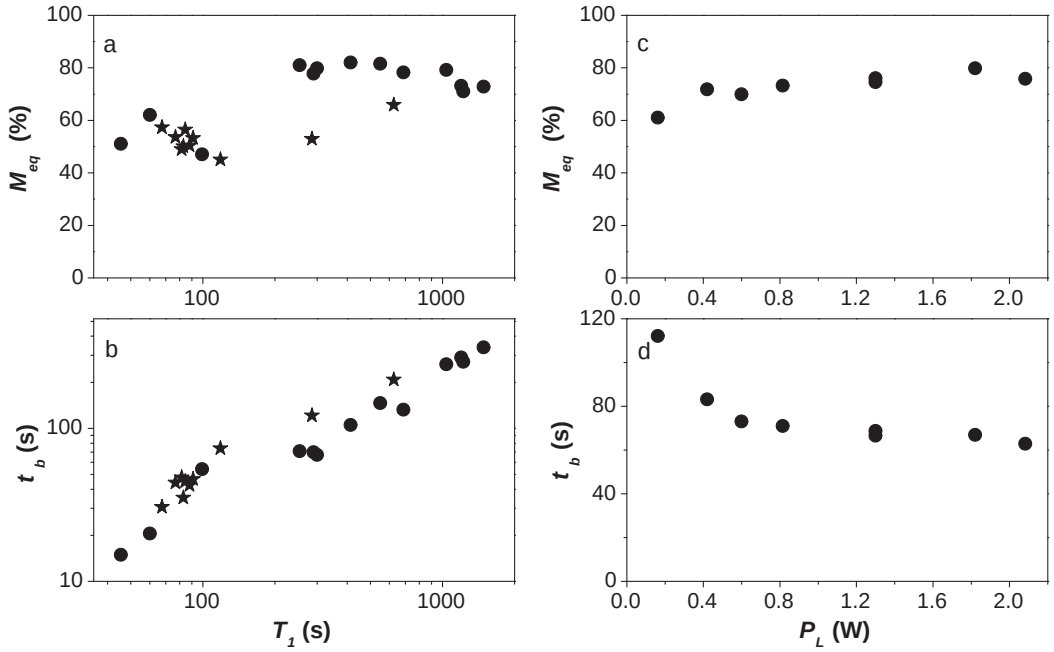

Figure 4: Results obtained at 1.5 T in the 1.33 mbar cell. (a): Steady-state polarization, and (b): Polarization build-up time constant, as a function of the discharge-induced decay time of the polarization T_1. Circles and stars: broadband (2 W) and single mode (0.5 W) pump lasers, both running at full power. (c): Steady-state polarization, and (d): Polarization build-up time constant, as a function of incident laser power $\mathcal{P}_L$. Data are obtained with the broadband pump laser and for T_1=300 s.

infers a steady-state polarization $M_{eq}=(1+2T_e/(\epsilon T_1))^{-1}$ and a build-up time $t_b=2T_eM_{eq}/\epsilon$. Using values of n_m and T_1 measured in the absence of pumping beam, the predicted polarization is $M_{eq}\simeq 1$, at all pressures. The build-up times are in the range 20-300 s for the low pressure cell, and in the range 15-40 s for the three high pressure cells. Although this elementary model is clearly not sufficient to predict M_{eq}, it accounts reasonably well for the observed dynamics. Its domain of validity and accuracy are estimated from detailed rate equations for the six 2^3S-sublevel populations. We find that in our experimental conditions and for the observed range of nuclear polarization, $2\langle I_z\rangle/\hbar$ given by the simple model differs from the exact value by a factor not exceeding 2, depending on M and on the gas pressure. This difference results from incomplete population transfer into (A_5,A_6) as well as from deviations of the order of ϵ of the populations a_5 and a_6 from their assumed spin-temperature values. In spite of its simplicity, the model sheds light on two key features: (*i*) The dynamics of optical pumping at 1.5 T is intrinsically limited by hyperfine decoupling. (*ii*) The build-up time, at least in the explored range of parameters, weakly depends on pressure and is affected only through changes of n_m and T_1.

For application purposes, production rates of polarized atoms per unit volume $R_a=PM_{eq}/t_b$ are compared to published results for standard MEOP conditions and similar sealed cells in Table 1. At low pressure, production rates at high field are lower than those obtained with low-field optical pumping. Nevertheless, one can take advantage of the weak pressure dependence of M_{eq} and t_b at 1.5 T to efficiently perform MEOP at higher pressure. By increasing the pressure from 1.33 to 32 mbar, a factor of 10 in R_a is gained and good production rates are recovered. For instance, gas in a 250 cc cell at 32 mbar can be polarized

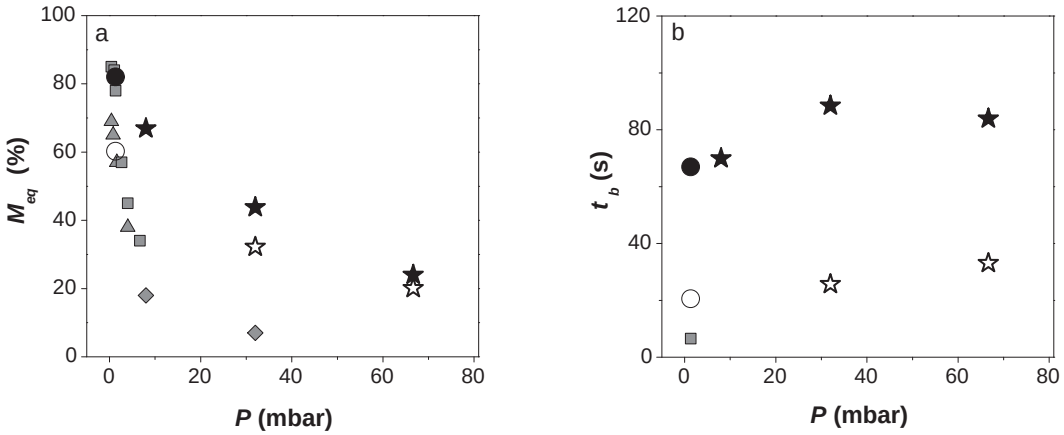

Figure 5: (a): Steady-state polarization, and (b): Polarization build-up time constant, as a function of ^{3}He pressure P, at high and low magnetic fields. Circles and stars are 1.5 T data obtained with a broadband (2 W) and single mode (0.5 W) pump lasers respectively. Filled (open) symbols are for weak (strong) discharge : T_1=300 (60), 2600, 1600 (325), and 1300 (700) s for 1.33, 8, 32, and 67 mbar, respectively. Triangles, squares, and diamonds are low-field data published in [5], [6], and [7] respectively (all for weak discharges).

at 40% within 3 minutes. This amount of gas is suitable for small animal lung imaging after compression to atmospheric pressure. For human lung MRI, considerable scaling-up or accumulation of polarized gas remains necessary. However, optical pumping around 50 mbar would considerably simplify the compression stage by reducing the compression ratio from 1:1000 down to 1:20.

An intrinsic advantage of the high-field MEOP scheme is that, due to the large Zeeman splittings in the 2^3S-2^3P transition, the magnetic sublevels involved in optical pumping are selected by the frequency of the light, and not only by its polarization. High-field MEOP is therefore extremely robust against polarization impurity of the pumping light. This is a crucial issue for massive production of polarized ^{3}He using high laser power, since imperfect light polarization can severely limit achieved polarizations at low field [14].

5 Perspectives

The nuclear polarization improvement observed at 1.5 T for high pressures is plausibly due to the inhibition by hyperfine decoupling of relaxation channels in atomic and/or molecular states in the plasma, as suggested by preliminary results at 0.1 T [7]. Further experiments at different magnetic field intensities are planned to confirm this hypothesis. In this perspective, the present study provides a first set of data showing that, in spite of the large hyperfine decoupling in the 2^3S state, MEOP at high field (*i*) still yields high nuclear polarizations at low pressures and (*ii*) extends the domain of its applicability to higher pressures, providing fair polarizations and high production rates. From a practical point of view, and in the perspective of a large scale medical use of polarized gases, the development of a ^{3}He polarizer operating at 1.5 T (a widely used magnetic field in MRI), and at tens of mbar (for simplified compression) could be an attractive choice.

Table 1: Steady-state polarizations M_{eq}, build-up times t_b and production rates R_a (see text) versus gas pressure P and laser power $\mathcal{P}_\mathcal{L}$ for the data in Fig.5 and other published data. Results in parenthesis correspond to strong discharges.

Ref	P (mbar)	$\mathcal{P}_L$ (W)	M_{eq} (%)	t_b (s)	T_1 (s)	R_a (mbar/s)
this work	1.33	2.0	80 (60)	67 (20)	300 (60)	0.016 (0.039)
this work	8	0.5	67	70	2600	0.076
this work	32	0.5	44 (32)	88 (26)	1600 (325)	0.159 (0.401)
this work	67	0.5	24 (20)	84 (33)	1300 (700)	0.191 (0.405)
[12]	1	0.05	50 (40)	40 (9)	270 (40)	0.013 (0.047)
[14]	1.33	1.1	56 (39)	11 (2)	400 (10)	0.066 (0.266)
[6]	1.33	4.5	78 (45)	6.5(0.3)	900 (15)	0.160 (2)

References

[1] Becker J. *et al.*, Nucl. Instrum. Meth. A, **402**, (1998), 327.

[2] Möller H. *et al.*, Magn. Res. in Medicine, **47**, (2002), 1029.

[3] Walker T. G. and Happer W., Rev. Mod. Phys., **69**, (1997), 629.

[4] Colegrove F. D., Schearer L. D. and Walters G. K., Phys. Rev., **132**, (1963), 2561.

[5] Leduc M., Crampton S. B., Nacher P.-J. and Laloë F., Nucl. Sci. Appl., **1**, (1983), 1.

[6] Gentile T. R. and McKeown R. D., Phys. Rev. A, **47** , (1993), 456.

[7] Nacher P.-J. *et al.*, Acta Phys. Pol. B, **33**, (2000), 2225.

[8] Chernikov S. V. *et al.*, Electron. Lett., **33**, (1997), 787.

[9] Tastevin G. *et al.*, Appl. Phys. B, **78**, (2004), 145.

[10] Courtade E. *et al.*, Eur. Phys. J. D, **21**, (2002), 25.

[11] Nacher P.-J. and Leduc M., J. Physique, **46**, (1985), 2057.

[12] Stoltz E. *et al.*, Appl. Phys. B, **63**, (1996), 629.

[13] with notations of [10], ϵ=$2sin^2\theta_+$=1×10^{-2} at 1.5 T.

[14] Leduc M., Nacher P.-J., Tastevin G. and Courtade E. Hyper. Interact., **127**, (2000), 443.